

# Gradient-Modulus PDMS-CNT Composite Materials for Robotic Tactile Perception

Yian Wen<sup>1</sup>, Junjie Weng<sup>1</sup>, Danping Zhang<sup>1</sup>, Cheng Huang<sup>1</sup>, and Silin Guo<sup>1,#</sup>

<sup>1</sup> College of Intelligence Science and Technology, National University of Defense Technology, Changsha, 410073, China  
# Corresponding Author / Email: silin7069@qq.com, TEL: +86-13006373791

KEYWORDS: gradient-modulus materials, flexible tactile sensing, porous structure

*Three-dimensional (3D) microstructures have attracted considerable attention due to their significant advantages in softness and compressibility, showing potential applications in biomedical monitoring, human-machine interaction interfaces and robotic tactile sensing. For flexible pressure tactile sensors, the mechanical properties of the structured dielectric layer play a crucial role in determining the performance of the sensor. Sensitivity and detection limit are important characteristics of pressure sensors which determines the ability to detect subtle pressures and usually depend on the deformation of the dielectric material under pressure: the greater the deformation, the higher the sensitivity, but the lower the detection limit. Increasing voids in the dielectric layer and enhancing its compressibility through microstructural engineering is an effective strategy for achieving high sensitivity in sensors. The presence of micropores makes the structure more compressible, significantly improving sensitivity compared to solid dielectric materials. However, this high sensitivity is limited to low pressure conditions due to Young's modulus constraints. Constructing gradient porous materials in layers is an effective way to address such issues, but the design and preparation of complex pores requires the further development of advanced or complex fabrication processes. This paper proposes a simple strategy for adjusting the mechanical properties of porous materials based on Polydimethylsiloxane (PDMS), using freeze-drying technology to prepare a carbon nanotube (CNT) conductive scaffold and introducing PDMS as a filling material. Negative pressure filling technique for localized filling of PDMS into the pores of the stent surface. The Young's modulus of the composite material displays a gradient distribution, with higher values around the periphery and lower values at the center, ensuring that the dielectric material can withstand higher pressure load and enables the pressure sensor to cover a wider pressure sensing range (0-1000 kPa) while maintaining high sensitivity.*

## NOMENCLATURE

$R$  = resistance value

$E$  = elastic modulus

## 1. Introduction

Flexible tactile sensors provide robots with tactile capabilities close to human skin, enabling fine manipulation and environmental adaptation, and are key components for robots to achieve interaction with the environment<sup>[1]</sup>. There are many sensing mechanisms for tactile sensors, including resistance, capacitance, piezoelectric, etc., among which piezoresistive tactile sensors have attracted considerable attention due to the ease of signal measurement and scalable fabrication process<sup>[2]</sup>. Usually, flexible sensors consist of electrodes with a dielectric layer, and the performance of flexible pressure tactile sensors is determined by the mechanical properties of the structured dielectric

layer. To achieve high sensitivity ( $>1 \text{ kPa}^{-1}$ ) and a wide sensing range ( $>10 \text{ kPa}$ ), researchers have chosen nanomaterials with excellent electromechanical stability, such as metal nanowires<sup>[3]</sup>, carbon nanotubes<sup>[4]</sup> and graphene<sup>[5]</sup> with micro- and nanostructures<sup>[6]</sup>. For example, Pan et al. provided the sensor graphene layer with gradient folded and porous structures through pre-stretching and laser reduction<sup>[7]</sup>, and Guo et al. enhanced the texture recognition capability of the sensor by further preparing folded microstructures on top of the interlocking structures<sup>[8]</sup>. This method of combining multiple microstructures can effectively improve the performance of the sensor, but it also places high demands on the preparation process of the materials.

Herein, this paper proposes a simple strategy for adjusting the mechanical properties of porous materials based on Polydimethylsiloxane (PDMS), using freeze-drying technology to prepare a carbon nanotube (CNT) conductive scaffold and introducing PDMS as a filling material. The resulting PDMS-CNT composite material (PCCM) exhibits anisotropic electrical conductivity, manifesting different force-resistance characteristics under normal and

tangential forces.

## 2. Materials and Methods

### 2.1 Materials

CNT with  $-COOH$  groups were obtained from XFNANO. Sodium alginate, calcium DL-lactate pentahydrate and glycerol were purchased from Sinopharm.

### 2.2 Synthesis of solution

First, sodium alginate powder was added into deionized water to form a 0.2% (w/v) alginate solution. Then, CNT were incorporated in alginate by homogenization (40 min., 25 °C) in a sonicator to form a 1mg/mL SA-CNT suspension. Set magnetic stirring 55 °C, 400rpm, gradually add calcium carbonate powder to deionized water to formulate a 1.5mol/L solution, the adding process as far as possible to keep the solution in a clear state. 20 mL of glycerin was added dropwise into 2 mL of calcium lactate solution with continued stirring (50°C, 400rpm). After completion, the temperature was adjusted to room temperature, the speed was increased to 500 rpm, and stirring was continued for 1 h.

### 2.3 Fabrication of CNT conductive scaffold

First, 1 mL of calcium lactate solution was dropped onto a plate. Then, 0.5 mL of SA-CNT suspension was dropped into the solution to form CNT-alginate hydrogels and set for 10 min. Next, the hydrogel was carefully washed with water several times. Finally, after the freeze-drying process, the CNT conductive scaffold (CNT-aerogel) was obtained. The fabrication process of CNT-aerogel is shown in Fig. 1(a).

### 2.4 Fabrication of PDMS-CNT Materials

First, the CNT aerogel was fixed using a jig and allowed to rotate slowly at 10 rpm, then the hardener (Sylgard 184B) was added to the solution at a weight ratio of 1:10. Using a pipette, 0.1ml of the prepared mixture was dropped onto the surface of the rotating stage and the stage was rotated for 1 minute to distribute the PDMS as evenly as possible over the surface. After stopping the rotation, the fixture was released and the vacuum created inside the scaffold by the removal of the applied pressure allowed the PDMS solution to enter the filled pores. Finally, the excess PDMS was removed with a scraper and the materials were placed in a drying oven heated at 80 °C for 2 h. The fabrication process of the PCCM is shown in Fig. 1(b).

### 2.5 Characterization and Testing Methods

The pressure performance testing was performed using a force testing machine (Zhiqu precision instruments ZQ990), and the electrical property was characterized by a resistance meter (0.1  $\mu\Omega$  to 1.2 G $\Omega$ , AT515, Changzhou Applent Instrument Co., Ltd.). The morphology of the PCCM was verified using a scanning electron microscope (SEM, ESCAN MIRA LMS). The chemical composition was investigated using a Raman spectroscopy (Horiba LabRAM HR Evolution at 633 nm).

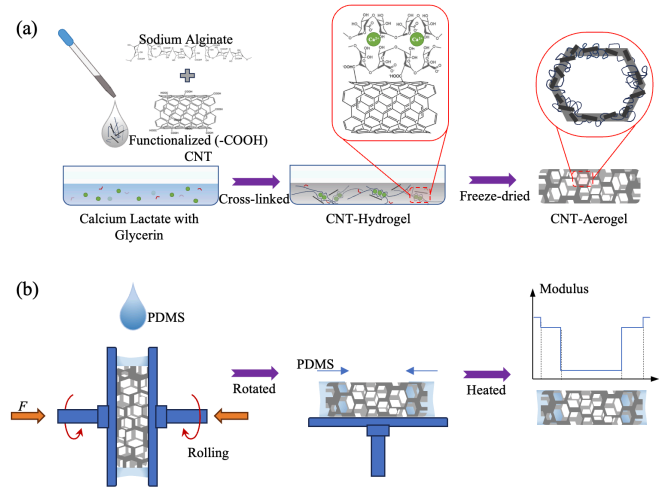


Fig. 1 Schematic illustration of fabrication of materials: (a) CNT conductive scaffold, (b) PCCM.

## 3. Results and Discussion

### 3.1 Characterization of the composite materials

The morphology of the PCCM were shown in Fig. 2. Images observed that the inner structure of the material presents pores. The thickness of the PDMS filling for the PCCM with a diameter of 5mm was approximately 0.3mm.

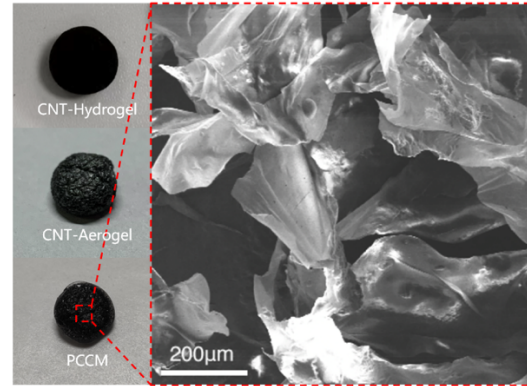


Fig. 2 Morphology of the composite materials

To confirm the presence of encapsulated CNT, the CNT-aerogel was analyzed with Raman spectra, as shown in Fig. 3. The increased intensity ratios of the D-peak and G-peak were obtained from the CNT-alginate which confirmed the incorporation of CNT within alginate after gelation. Because of lyophilization, the band corresponding to water in the Raman spectra was low.

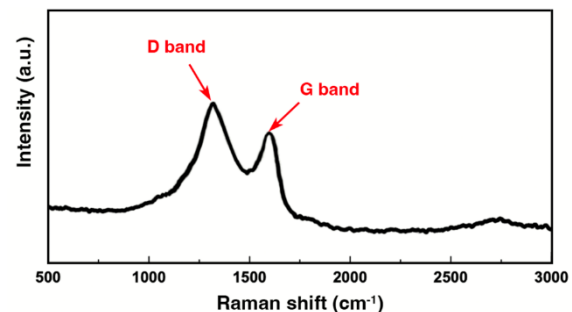


Fig. 3 Representative Raman-spectra of the CNT-alginate

### 3.2 Pressure Sensing Performance of the PCCM

As the resistance change  $\Delta R/R_0$  can evaluate the sensing performance, we fabricated a pressure sensor based on the PCCM, which used two stripes of copper foil as electrodes. For performance comparison, we also fabricated another pressure sensor based on the CNT-aerogel. The response properties of sensors under increasing pressure are demonstrated in Fig. 4(a). Under low pressure loading ( $<50\text{kPa}$ ), the sensor based on CNT-aerogel exhibited better sensitivity, while under high pressure ( $>100\text{kPa}$ ), the PCCM-based sensors exhibits better and also had a wider operation range. When a tangential force was applied to the PCCM-based sensor, the force-resistance characteristics of PCCM—based sensor was similar with the pressure sensor based on CNT-aerogel.

The PCCM-based sensor also exhibits excellent stability and reliability in the sensing performance. For repeated applied 150kPa pressure, the PCCM sensor could successfully endure different repeated frequency of this high pressure loading and unloading, as shown in Fig. 4(b), exhibiting the excellent reliability and repeatability.

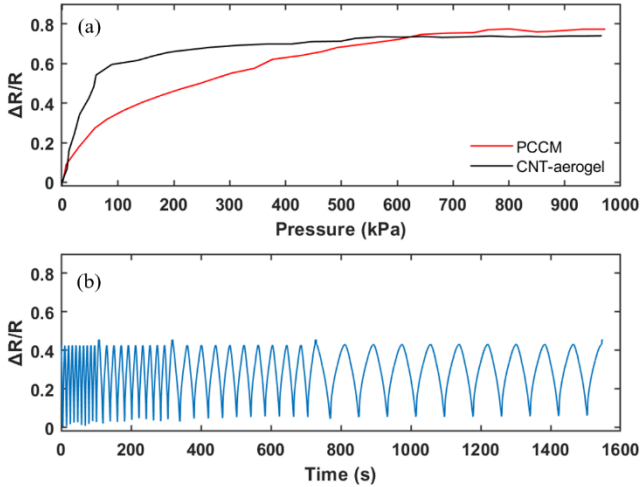


Fig. 4 Electromechanical response of the PCCM-based pressure sensor: (a) Pressure- $\Delta R/R$  curves for the pressure sensors. (b) Response curves of different repeated frequency with the 150 kPa.

### 3.3 Force Model and Circuit Model of the PCCM

To further explore the force-responsive mechanism of the PCCM sensor, theoretic model and computational analysis are investigated from the sensor structure. Fig.5 schematically illustrates the processes of the materials being pressed under different pressures. As shown in Fig. 5(a), the CNT-aerogel has a massive air-gap porous structure. When the pressure is applied, the air gaps compressed and the skeletons started to come into contact, which increase the contact area and sensitively reflect in current change. With the increase of pressure, the contacting area constantly increases but slowly due to the mechanism strength of CNT-aerogel with single-modulus.

PCCM has the same conductive circuit as CNT-aerogel. Since the PDMS fills the pores, it makes the PCCM edges have a different mechanistic strength than its center part, and it can resist the pressure better. As shown in Fig. 5(b), under the same pressure, the compression of PCCM is smaller than that of CNT-aerogel, which reduces the sensitivity at low pressure, but improves its pressure resistance and

widens the response range.

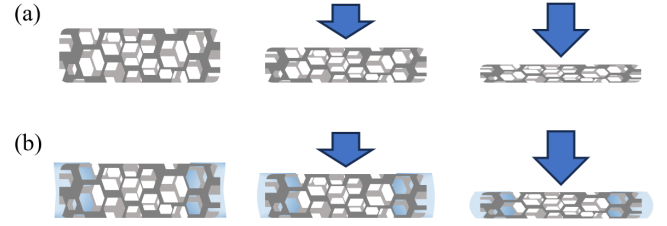


Fig.5 Schematics of structural change of (a) the CNT-aerogel and (b) the PCCM under different pressures.

Therefore, to better characterize the force-resistance characteristics of PCCM, the circuit model shown in Fig. 6(a) is constructed, which is determined by equation (1)

$$R_{AB} = \frac{2R_{CP}R_C + R_C R_P}{2R_{CP} + R_P + 2R_C} \quad (1)$$

where each resistance  $R$  is related to the mechanical properties of the material,  $R \propto E$ . The force simulation analysis of the material is carried out by setting the Young's modulus of CNT-aerogel to 2.9 MPa and Poisson's ratio to 0.2, and the Young's modulus of PCCM edge (thickness of 0.3 mm) to 15 MPa and Poisson's ratio to 0.49 with reference to the material properties of PDMS. It can be seen from Fig. 6(b) that, at the same pressure, the edge layer of PCCM generates a greater stress in order to resist the external forces, which making the deformation of the center region, which is dominant in the resistive model, smaller than that of the CNT-aerogel.

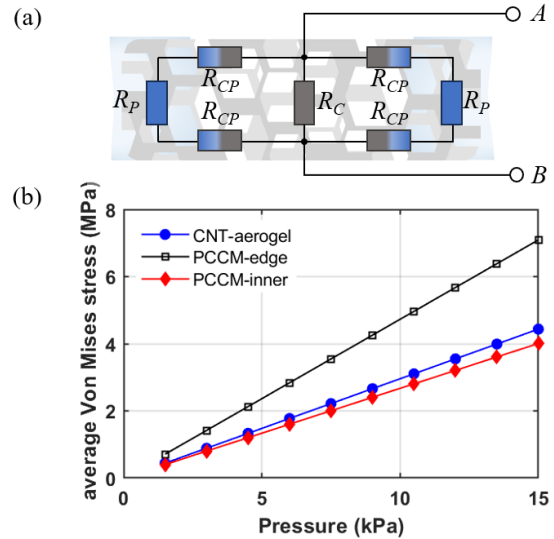


Fig.6 (a) Circuit model for the sensor based on PCCM. (b) Simulation curves for the average Von Mises stress of the sensors based on PCCM and CNT-aerogel under tiny working pressure.

## 4. Conclusion

In this paper, a method for the preparation of modulus PDMS-CNT composites is proposed. Based on CNT conductive scaffold prepared by sodium alginate and CNT with -COOH, PDMS is further selected as filler material to realize the gradient distribution of Young's modulus of the composite material. The pressure sensor based on the gradient-modulus PDMS-CNT composite materials presents a wide operation

range of up to 1000kPa. The feasibility of the material for robotic haptic sensing is verified by testing the pressure sensing performance of the material and constructing the force model and circuit model.

## ACKNOWLEDGEMENT

This work was supported by the Hunan Provincial Natural Science Foundation of China (Grand No. 2024JJ6476).

## REFERENCES

1. Wang, C., Liu, C., Shang, F. et al., "Tactile Sensing Technology in Bionic Skin: A Review," *Biosens Bioelectron*, Vol. 220, p. 114882, 2023.
2. Xu, Z., Wu, D., Chen, Z. et al., "A Flexible Pressure Sensor with Highly Customizable Sensitivity and Linearity Via Positive Design of Microhierarchical Structures with a Hyperelastic Model," *Microsyst Nanoeng*, Vol. 9, p. 5, 2023.
3. Shen, G., Huang, W., Li, H. et al., "Highly Stable Capacitive Tactile Sensors with Tunable Sensitivity Facilitated by Electrostatic Interaction of Layered Double Hydroxide, Mxene, and Ag Nws," *Science China Technological Sciences*, Vol. 66, No. 11, pp. 3287-3297, 2023.
4. Chen, D., Zhang, T., Geng, W. et al., "An Intelligent Tactile Sensor Based on Interlocked Carbon Nanotube Array for Ultrasensitive Physiological Signal Detection and Real-Time Monitoring," *Advanced Materials Technologies*, Vol. 7, No. 11, p. 2200290, 2022.
5. Siskins, M., Lee, M., Wehenkel, D. et al., "Sensitive Capacitive Pressure Sensors Based on Graphene Membrane Arrays," *Microsyst Nanoeng*, Vol. 6, p. 102, 2020.
6. Tan, Y., Liu, X., Tang, W. et al., "Flexible Pressure Sensors Based on Bionic Microstructures: From Plants to Animals," *Advanced Materials Interfaces*, Vol. 9, No. 5, 2022.
7. Lv, Y., Zhang, M., Zhao, B. et al., "Flexible Laser-Reduced Graphene with Gradient-Wrinkled Microstructures for Piezoresistive Pressure Sensors," *ACS Applied Nano Materials*, Vol. 7, No. 16, pp. 18986-18994, 2024.
8. Bai, N., Xue, Y., Chen, S. et al., "A Robotic Sensory System with High Spatiotemporal Resolution for Texture Recognition," *Nat Commun*, Vol. 14, No. 1, p. 7121, 2023.